# UBE2N: Hope on the Cancer Front, How to Inhibit This Promising Target Prospect?

Florian Schwalen, Côme Ghadi, Léonie Ibazizene, Shafi Ullah Khan, Jana Sopkova-de Oliveira Santos, Louis-Bastien Weiswald, Anne Sophie Voisin-Chiret, Matthieu Meryet-Figuiere, Charline Kieffer

# UBE2N: Hope on the cancer front, how to inhibit this promising target prospect?

*Florian Schwalen,[a,b] Côme Ghadi,[a] Léonie Ibazizene,[c,d] Shafi Ullah Khan,[c,d] Jana Sopkova-de Oliveira Santos,[a] Louis-Bastien Weiswald,[c,d] Anne Sophie Voisin-Chiret,[a] Matthieu Meryet-Figuiere,[c,d,*] Charline Kieffer [a,*]*

** corresponding authors*
*a. Université de Caen Normandie, CERMN UR4258, Normandie Univ, F-14000 Caen, France*
*b. CHU Caen Normandie, Pharmacie, 14033 Caen, France.*
*c. Normandie Univ, Université de Caen Normandie, Inserm U1086 ANTICIPE (Interdisciplinary Research Unit for Cancer Prevention and Treatment), 14076 Caen, France*
*d. Comprehensive Cancer Center François Baclesse, UNICANCER, 14076 Caen, France*

## ABSTRACT

UBE2N protein belong to the UE2s family and play a crucial role in DNA repair, making it an exciting target for the development of innovative anti-cancer therapies. With the aim of discovering UBE2N inhibitors (UBE2Ni), this perspective seeks to review and provides elements to guide the design of new compounds. We propose a chemo-informatic structural analysis of the protein and its areas of interaction with its different partners. While covalent UBE2Ni are the most advanced molecules in their development, non-covalent inhibitors offer significant advantages that could overcome the limitations of covalent ones, particularly in terms of selectivity. Lastly, to obtain a drug candidate, early assessment of the druggability of compounds is essential in a hit to lead process. For existing UBE2Ni, a critical challenge lies in their pharmacokinetic properties and will obviously have to be considered as early as possible to hope for an application in human therapy.

## KEYWORDS

cancer, DNA repair, UBE2N, pharmacological inhibitors, drug design

## SIGNIFICANCE

- Comprehensive overview of the role of UBE2N and its potential as a therapeutic target
- Analysis of the key protein-protein interactions carried out by UBE2N and molecular interfaces engaged
- Comparison of the different class of UBE2N inhibitors (UBE2Ni) and understanding of the mechanism of covalent inhibitors
- Highlight of the key points to consider and provide clues to guide medicinal chemists designing UBE2Ni

## INTRODUCTION

### ***UE2S Family***

Ubiquitin-conjugating enzymes 2 (UE2s) play a central role in the in the attachment of ubiquitin (Ub) to cellular proteins. They interact with an E1 enzyme and one or more E3 ligases. In the Ub transfer pathway, E1 transfers ubiquitin to UE2 and next ubiquitin is transferred onto a specific set of substrates, with the assistance of an E3 ubiquitin ligase, an essential cofactor in the ubiquitin transfer process and its target selectivity.

As of now, approximately 40 UBE2 enzymes have been identified. The majority are involved in ubiquitination processes, with a few exceptions: UBE2F and UBE2M participate in neddylation, UBE2I is involved in SUMOylation, and UBE2L6 plays a role in ISGylation.[1] All UE2s members fulfill their function *via* a key cysteine residue which is conserved among the family. Most of UE2s enzymes have between 150 and 250 residues, but some of them, such as UBE2O, can reach 1290 residues (figure 1.A.). Despite this difference in size, the three-dimensional (3D) structures of the domain of about 150 residues bearing the conserved key cysteine are similar among family members (figure 1.B.C.D.) and the spatial position of the conserved cysteine (Cys87 in UBE2N) is close in all solved structures of UE2s (figure 1.C.). The 3D structure of conserved domain includes five α-helices (α1–α5) and four β-strands, which form a single antiparallel β-sheet (Figure 2.A). The major differences among the UE2s members are observed in the α2-α3 loop which varies in length as well as in position (figures 1.E.F.). Moreover, the solved 3D structures also highlighted different positions of α4 and α5 helices in UBE2Q1 (figure 1.E. brown), UBE2Q2 (figure 1.E. deep teal) and UBE2N (figure 1.E. green).

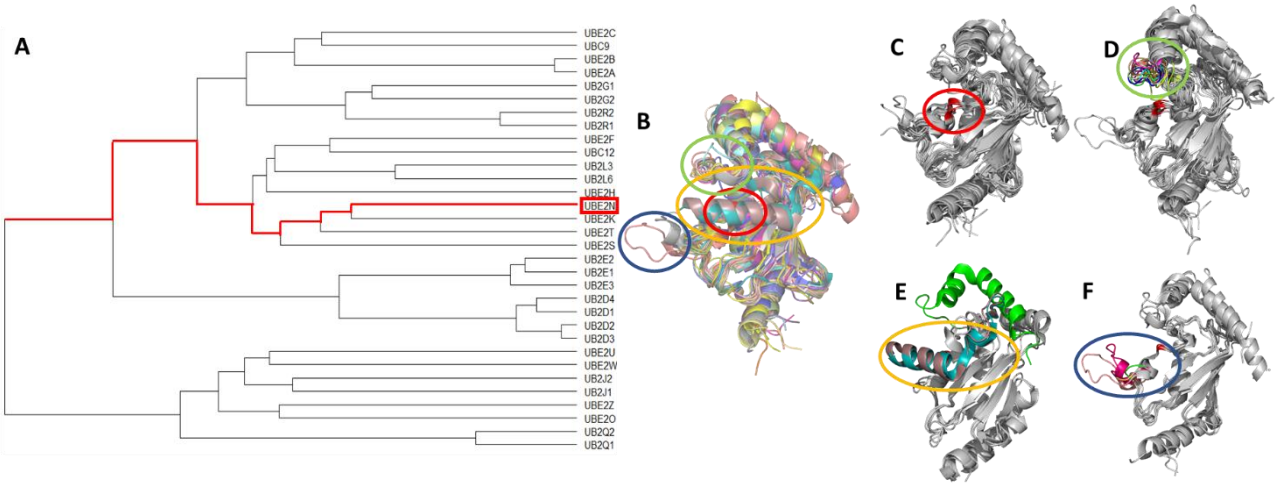


*Figure 1. Ubiquitin-conjugating enzyme E2 family (UE2). (A) Cladogram representing the UE2 family, constructed from sequence alignment data using Clustal Omega.[2] (B) Alignment of the 3D structures of UE2 family members. (C, D) Structural similarities between members of the UE2 family and (E, F) structural differences between UBE2N and other UE2 family members. The red circle in (B, C) highlights the conserved cysteine residue characteristic of UE2 enzymes. The green circle in (B, D) indicates a conserved flexible loop responsible for modulating the active site cavity. The yellow circle in (B, E) emphasizes differences in the positions of the α4 and α5 helices among UBE2Q1 (brown), UBE2Q2 (deep teal), and UBE2N (green). The blue circle in (B, F) denotes the variable length of the α2-α3 loop.*

In addition to their role in the Ub process, UE2s perform a variety of functional functions.[3]

Given that, they are considered as potential therapeutic targets, particularly in cancer treatment, but only a limited number of UE2 inhibitors are currently under development and always as an early-stage.[4] Moreover, based on a wide range of substrates and functions that are affected by E2s, relevant *in vivo* models for assessing these molecules are awaited for further development. Interestingly, despite their common functions in Ub pathway, the distinct regions in E2s are involved in many protein-protein interactions, raising the possibility of additional modes of inhibition.[5]

This perspective will focus on UBE2N (also known as Ubc13), as a really interesting potential target for cancer treatment. A single review described UBE2N in cancer processs,[6] but did not consider the development and design of specific inhibitors In addition to a description of UBE2N and its various functions, we propose an unpublished chemoinformatic work that determine the interaction surfaces of UBE2N with its various partners, to guide researchers wishing to design new UBE2Ni. This will be followed by a review of existing UBE2Ni, including their advantages and their limits, and an analysis of their druggability. Finally, we will outline the key points that need to be taken into account in order to design new and more potent UBE2Ni.

## ***UBE2N an ubiquitin conjugating enzyme with many functions***

UBE2N is an E2 ubiquitin ligase that catalyses the formation of ubiquitin chains on various substrates. Protein ubiquitination is mainly known for its role in the control of protein degradation, when the lysine 48 (K48-linked poly-Ub chain is anchored target proteins. On the other hand, UBE2N catalyses the formation of poly-Ub chains linked *via* K63[7], which is not a signal for protein degradation but rather plays a variety of regulatory roles, for example in cellular signalling,[8,9] protein trafficking,[10,11] or in HR (Homologous Recombination) DNA repair.[12] More specifically, the K63 ubiquitination mediated by UBE2N has been reported to function in DNA repair,[12] NF-κB signaling[13] and β-amyloid plates accumulation.[14]

When it is localized in the nuclear compartment, in complex with UBE2V2 (also known as Mms2), UBE2N promotes the ubiquitination of histone H2A[15] at the sites of DNA double-strand breaks, leading to the recruitment of repair proteins RAP80 and eventually of BRCA1 to the DNA lesions, thus allowing HR DNA repair to take place.[12,13]

UBE2N also acts in association with UBE2V1 (also known as Uev1a) and the TRAF6 E3 ligase in the cytoplasm, thereby controlling IKK (IκB kinase) activity through K63 ubiquitination.[13] As a result of IKK activation, NF-κB is itself activated, leading among other roles to the upregulation of factors limiting antitumoral immunity such as PD-L1 (Programmed Death-Ligand 1).[16,17]

## ***Targeting UBE2N in therapeutic***

To date the majority of studies aiming to inhibit UBE2N activity have been held in the context of cancer. UBE2N overexpression has been shown to correlate with poorer survival in ovarian cancer [18] or AML (Acute Myeloid Leukemia)[16] for instance, and UBE2N inhibition has been explored in several cancer models.[19,20,21] In most studies, UBE2N inhibition has been considered as a monotherapy for its cytoplasmic functions (in association with UBE2V1) in NF-κB signaling pathway,[19,20] whose inhibition impairs cancer cells survival.

The nuclear functions of UBE2N (in association with UBE2V2), and its effects on DNA repair, have been less studied as an anticancer option.[22] While the HR DNA repair perturbation resulting from UBE2N inhibition can have an anticancer effect on its own, it should be expected to really shine in combination with DNA damaging therapies, such as radiotherapy,

platinum agents or PARP inhibitors (PARPi). Indeed, UBE2N downregulation or inhibition does sensitizes to radiation in breast cancer cells,[23] or to carboplatin in ovarian cancer-derived tumor organoids.[22] Also, higher expression of UBE2N is associated with lower response rate to a PARP inhibitor/Carboplatin combination in breast cancer patients,[22] further underlining the interest of targeting UBE2N to sensitize DNA damaging agents, which are most often used in cancer treatments.

Interestingly, the association of DNA damaging drug and HR DNA repair impairment by inhibition of UBE2N nuclear functions will increase genome instability, thus inducing neo-antigen presentation and boost antitumoral immunity. One of the main ways for cancer cells to escape antitumoral immunity is through the expression of PD-L1 membrane receptor, whose expression depends on UBE2N cytoplasmic regulation of NK-kB.[17] In this context, the dual role of UBE2N means that the consequences of its inhibition would act synergistically, creating a "perfect storm" against cancer cells.

Another recently described function of UBE2N-mediated ubiquitination is its ability to promote β-amyloid accumulation in mouse brains, while UBE2N levels are elevated in Alzheimer patients compared with healthy control.[14] In this context, K63 ubiquitination is proposed to replace K48, thus preventing proteasome degradation and therefore allowing accumulation of undegraded products.[24] UBE2N inhibition could thus be proposed as an interesting lead limit and/or delay the onset of Alzheimer disease, and future studies on this topic will be awaited with great interest.

## UBE2N: STRUCTURE, PARTNERS AND INTERACTION SURFACES

In addition to its canonical mechanism, UBE2N requires the help of E2 cofactors which have lost ubiquitin transfer activity: UBE2V2 in the nuclear compartment, and UBE2V1 in the cytoplasm.

UBE2N is composed of 152 amino acids with a molecular mass of approximately 17 kDa, corresponding to the conserved domain of ubiquitin-conjugating enzymes (UBEs). Structural data from solved 3D models of UBE2N, available in the PDB database, have been critical in mapping its interaction zones with various binding partners (Figure 2.B). UBE2N interacts with a wide range of proteins, including E3 ligases (ZNRF1, LNX1, RNF4, RNF8, TRIMs, TRAF6), ubiquitin, a stress response protein (STIP1), and two essential E2 cofactors UBE2V2 in the nucleus and UBE2V1 in the cytoplasm.

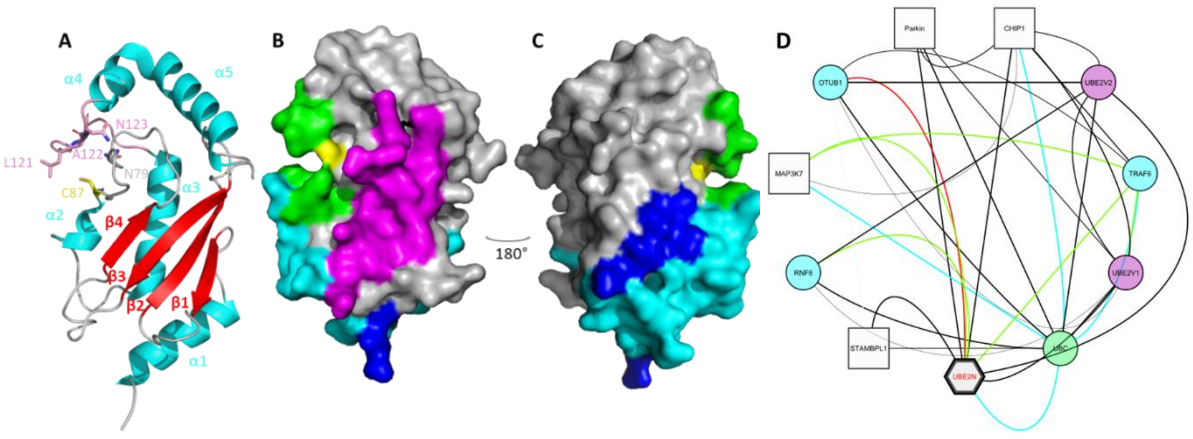

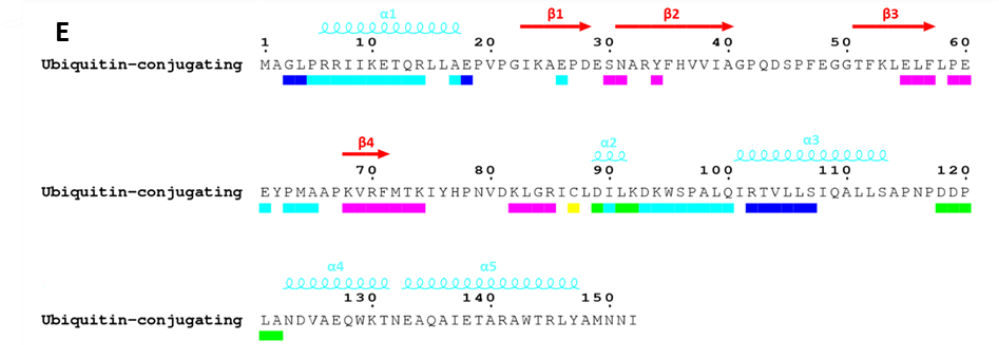


*Figure 2. 3D structure of UBE2N and its interactions with various partners. (A) Cartoon representation of UBE2N structure (PDB ID: 4ONN) coloured according to secondary structure elements, α-helix in cyan and β-strand in red, the side chain of residues discussed in manuscript are represented in stick. (B,C) Two views of surface representations with mapping of UBE2N interaction with its various partners: in magenta zone interacting with UBE2V2 and UBE2V1, in green with Ubiquitin, in cyan with E3 ligases and tumoral factors and in blue with bacterial proteins. OTUB1 inhibitor was found bound either in cyan region or magenta one in the solved complex structures. D) Interactome of UBE2N generated by Stitch.[25] The edges are coloured according to their function: inhibition (red), activation (green), catalysis (cyan), no information (black). The nodes are coloured in the same colour as the one used to colour the interaction surface deducted from the experimental complex structures. UBE2N is represented as a hexagon and the protein partners either as ellipse, when the structural data on complexes are available, or as rectangle in absence of complex structural data. (E) The UBE2N sequence. The residues presented on the interacting surfaces with various partners are coloured in same colour code as on A, B, C.*

The interaction surfaces of UBE2N with its cofactors UBE2V2 and UBE2V1 are identical (highlighted in magenta in Figures 2.B and 3.A). Both cofactors show minimal structural and sequence differences, with 89% sequence identity and a 94% similarity score (Figure 3.B). Their 3D structures are highly similar, with non-conserved residues between UBE2V2 and UBE2V1 located outside the UBE2N interaction surface (Figure 3.A). The Root-Mean-Square Deviation (RMSD) calculated for the Cα atoms of UBE2V2 and UBE2V1 is 0.454 Å. Consequently, inhibitors that target UBE2N's interaction with UBE2V2 would likely also affect its interaction with UBE2V1. In a view to design anti-cancer molecules, this lack of selectivity could be advantageous, due to the respective functions of these two cofactors, leading to a synergistic anticancer activity, as described below.

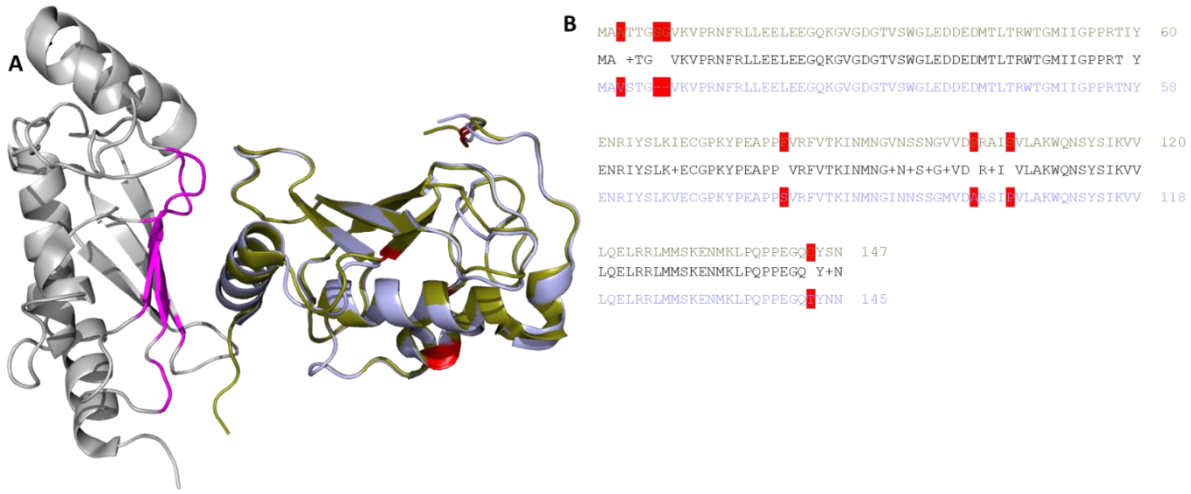


*Figure 3: Comparison of the two UBE2N partners, cytoplasmic UBE2V2 (orchid) and nucleic UBE2V1 (olive), differences in their sequences are highlighted in red in figure A and B.(A) Superposition of the 3D structures of UBE2N/UBE2V2 complex (PDB ID: 2C2V) on UBE2N/UBE2V1 one (PDB ID: 4ONL). The interaction pocket on UBE2N with both partners is coloured in magenta. (B) Alignment of UBE2V1 and UBE2V2 sequences [26] with the consensus sequence in black.*

The UBE2N active site, centered around Cys87, is highlighted in green in Figure 2.B and was identified from PDB structures of UBE2N complexed with ubiquitin (Cys87 is colored yellow in Figures 2.B and 2.C). The shape of the active site near Cys87 is influenced by the movement of a flexible loop comprising amino acids 114–124, which can adopt different conformations, altering the volume and shape of the active site cavity. To illustrate this, three examples of loop conformations in UBE2N, derived from the X-ray structures 4ONM, 3HCU, and 6UMP, are shown in Figure 4. The loop can be divided into two distinct parts: the first, spanning residues 114–116, is relatively less mobile, stabilized by hydrogen bonds between the backbone atoms of D118 and the side chain of N79. The second part, comprising residues 117–124, is highly mobile. The α4 helix, which follows this loop, varies in length and influences the flexibility of N123 and the conformation of this portion of the loop appears to be guided by interactions involving N123 and its neighboring residues. In the 3HCU structure, N123 is incorporated into the α4 helix, and its side chain does not participate in any notable interactions. The loop adopts a closed conformation, maintained by a salt bridge between D118 and K130. In contrast, in the 4ONM structure, the α4 helix is shorter, leaving N123 positioned at the helix terminus. Here, N123 engages in electrostatic interactions through its carboxylic acid group with V125, V80, and H77. This results in an intermediate loop conformation. Finally, in the 6UMP structure, the α4 helix loses a turn, significantly altering the local environment of N123. This change dramatically reshapes its interactions, with N123 now engaging with P78 and V125, ultimately leading to an open loop conformation.

We observe that the conformation of the loop significantly influences the shape and position of druggable pockets around Cys87 (Fig. 4B). In the structure co-crystallized with a covalent inhibitor (4ONM), three druggable pockets were identified.[27] Among them, a small pocket (pocket A) forms near Cys87 to accommodate the attached moiety, with a druggability score of 0.35 ± 0.09. This pocket is separated by a bridge from two larger adjacent flat pockets: pocket A' (druggability score = 0.53 ± 0.09) and pocket B' (druggability score = 0.77 ± 0.05). These bridges likely restrict the binding of larger inhibitors in this structure (Fig. 4B). In contrast, no druggable pocket was detected around Cys87 in the 3HCU structure. The closest pocket to Cys87 is pocket A, with a druggability score of 0.79 ± 0.007. Conversely, in the 6UMP structure, a large druggable pocket A encompassing the Cys87 and its vicinity was identified, with a druggability score of 0.79 ± 0.07. Although this pocket is larger, it is still divided into two regions by a bridge. Furthermore, the location, shape, and size of these pockets are accompanied by changes in the amino acids lining their surfaces (Fig. 4C). These observations highlight that the flexibility of the loop plays a critical role in modulating pocket properties and may have a significant impact on the design of UBE2N inhibitors.

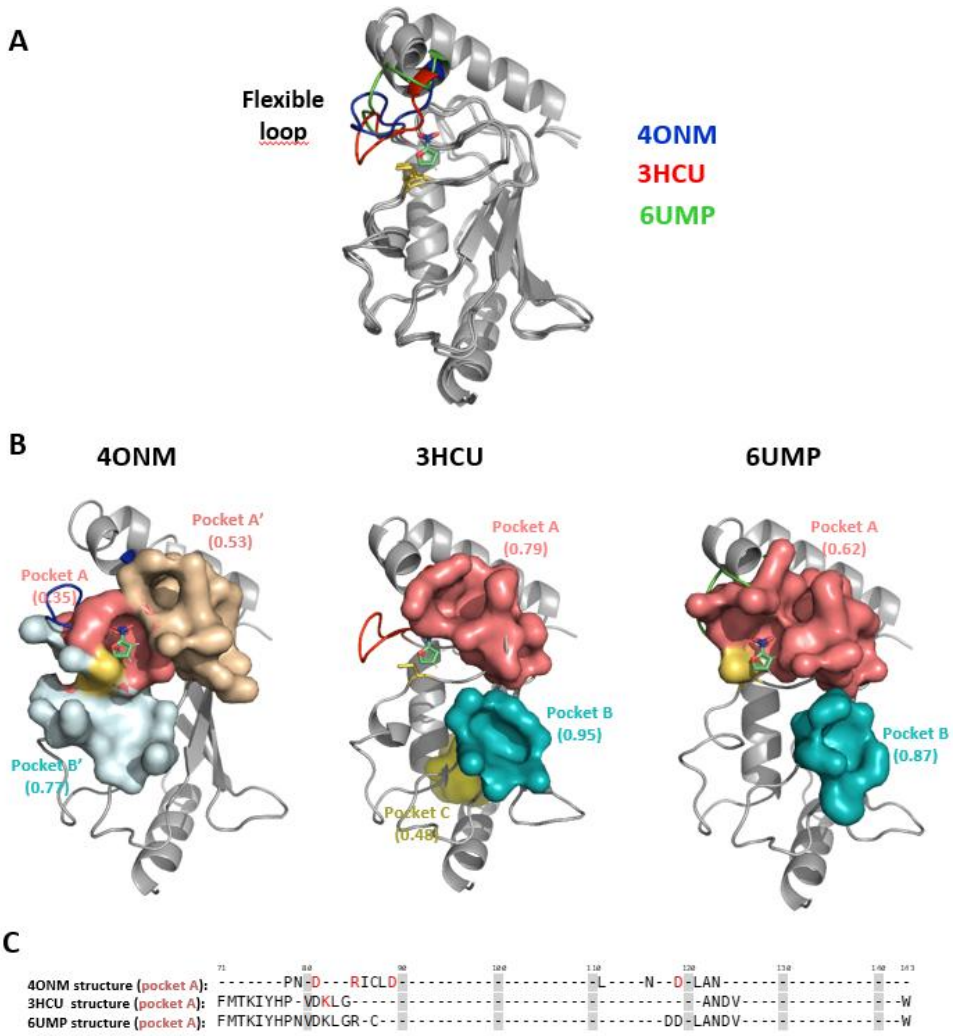


*Figure 4. Flexibility of the interface interacting with ubiquitin and covalent ligands illustrated using 3 structures of UBE2N – 4ONM, 3HCU, and 6UMP. (A) Illustration of the movement of the flexible loop (114-124) modifying the interaction surface. The ligand (colored in green) and cysteine residue (colored in yellow) are represented in stick. (B) Druggable pockets detected in each of the three structures were identified using PockDrug[27], with the predicted druggability scores indicated in brackets. (C) Amino acid composition of the principal druggable pockets detected near Cys87. Amino acids with charged side chains exposed on the protein surface are highlighted in red.*

Published data showed that UBE2N activity can be regulated by protein inhibitor OTUB1, synthetic covalent inhibitors, or non-covalent inhibitors. However, structural data on their mechanisms of action remain limited. To date, four structures of UBE2N co-crystallized with the deubiquitinating enzyme OTUB1 have been published[28,29] along with two structures of UBE2N bound to covalent inhibitors: NSC697923 (PDB ID: 4ONM) and BAY 11-7082 (PDB ID: 4ONN).[30] No structure UBE2N co-crystallized with a synthetic non-covalent inhibitor has been solved to date. X-ray structures show that OTUB1 can bind either to the UBE2V2/UBE2V1 binding site or to the E3 ligase binding site, but its precise mode of action remains unclear.

The interest in X-ray structures of UBE2N with covalent inhibitors is also limited. For example, NSC697923 binds to UBE2N *via* a covalent bond with Cys87, but in the 3D structure, only the 5-nitrofuran moiety added to the sulfhydryl group of Cys87 is visible.[30] As previously noted, a conformational change occurs in the loop between amino acids 114–124, creating a cavity that accommodates the attached moiety of the covalent ligand (Figure 4).

The nitrofuran moiety of NSC697923, observed in the crystal structure, lodges in this cavity and forms a hydrogen bond with Asn123. Similar results were observed for BAY 11-7082, another covalent UBE2Ni, in which the prop-2-enenitrile moiety binds to the sulfur atom of Cys87 and occupies the same cavity.

However, this cavity is too small to accommodate non-covalent inhibitors. Currently, no structural or modeling data are available regarding the interaction mode or binding site of non-covalent inhibitors targeting UBE2N.

## UBE2N INHIBITORS

### ***Covalent UBE2N inhibitors***

Three structurally distinct covalent inhibitors targeting UBE2N are described in the literature (figure 5). Despite their structural diversity, these molecules share a key feature: they all act as Michael acceptors due to their electrophilic properties. The mechanism of action of these compounds relies on the formation of a covalent bond with the nucleophilic Cysteine 87 residue onto UBE2N *via* a Michael addition mechanism. Indeed, the cysteine thiol is highly reactive due to its high electron density and polarizability (figure 6).

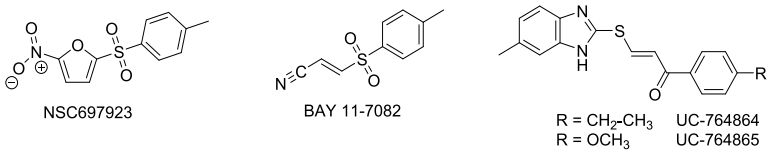


*Figure 5. UBE2N covalent inhibitors from literature.*

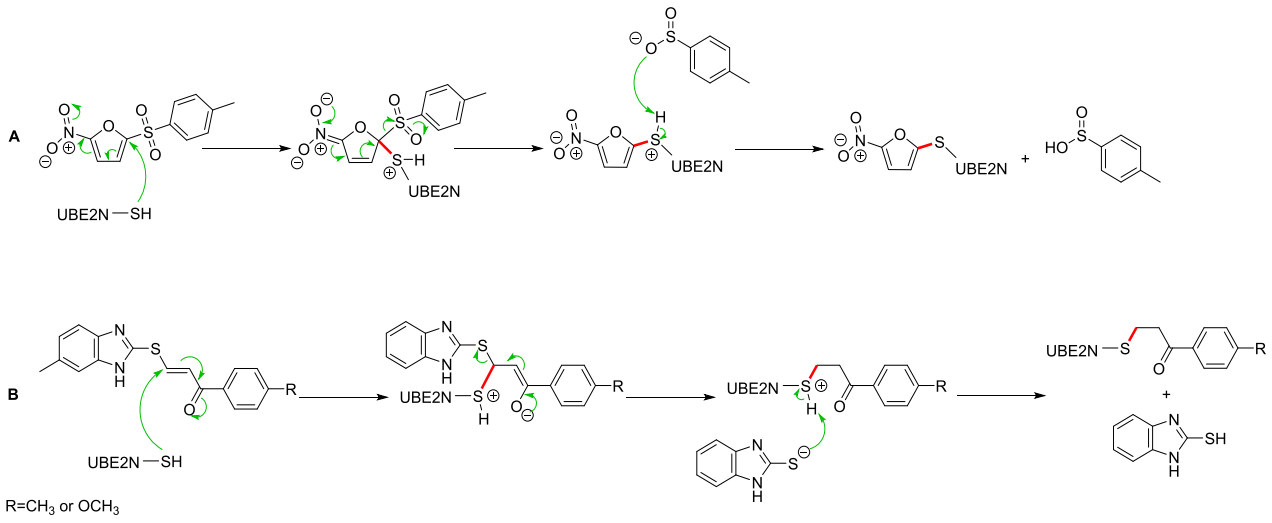


*Figure 6. Mechanism of covalent bond (red line) formation between UBE2N and UBE2N inhibitors NSC697923 and UC–764864/65 involving a Michael Addition reaction. A) NSC697923 is a nitroalkene Michael acceptor. B) UC-764864/65 possesses an α-β unsaturated carbonyl group.*

**BAY 11-7082** was firstly described in 1997 by Pierce *et al.*[31] for its NF-κB inhibitory activity, but its mechanism of action had not been elucidated. Because of its anti-inflammatory properties, it has been studied in several models with multiple potential therapeutic applications.[32,33,34,35]

In 2013, Strickson *et al.*[36] made a significant contribution in demonstrating the activity of the BAY 11-7082 on the poly-ubiquitination activity of UBE2N. The molecule is a Michael acceptor containing a *para*-methylphenylsulphonyl scaffold linked to a nitrile function by an ethylenic linker. BAY 11-7082 reacts with the sulfhydryl group of UBE2N-Cys87 through a Michael addition which leaves a prop-2-enenitrile moiety on the Cys87 sulphur atom.[30] However, the covalent binding is not specific to UBE2N. The molecule thus binds to other E2 ligases [36,30] but also to other targets, leading to many off-target effects.[35,37,38] Several publications have demonstrated *in vitro* cytotoxic activity of BAY 11-7082 in colon cancer,[39] gastric cancer [40] or lymphoma cells.[41] Thus, while BAY 11-7082 remains a tool for the realization of basic biology work, there is little chance that it will ever become an anticancer drug of choice.

**NSC697923** was identified as a UBE2N/UBE2V1 disruptor from a chemical library of 879 small molecules compounds by Pulvino *et al.* [20] In a first screening test, the inhibition of NF-κB activation in DLBCL (Diffuse large B-cell lymphoma) cells lines was measured using NF-κB luciferase-based reporter assay. Then, a structure-activity relationship (SAR) study was conducted and highlighted the decisive but not sufficient role of the nitrofuran moiety. The most promising molecule (NSC697923) is composed of a nitrofuran unit linked to a *para*-methylphenylsulfone moiety, such as BAY 11-7082. The Michael addition reaction is made *via* the only cysteine residue of UBE2N: the electrophilic sulfhydryl group of UBE2N-cystein 87 attacks the α-unsaturated carbon of the sulphone, leading to the formation of a nitrofuran adduct on the targeted protein and the departure of sulfinic acid. (figure 5A)

The selectivity of NSC697923 was then extensively studied by Hodge *et al.*[30] After developing an UBE2N mutant which resists to NSC697923 inhibition, the authors showed that the inhibition of DNA damage repair and NF-κB signalling by NSC697923 is largely due to a specific UBE2N inhibition. Thanks to the resolution of the co-crystal structure of the UBE2N-UBE2V2-NSC697923 complex structure, they showed that the specificity is due to the cysteine adduct which docks into an adjacent cleft that is absent in many other ubiquitin conjugating enzymes. More precisely, mutations modified the $\alpha$3-$\alpha$4 loop conformation and Leu121 side chain was placed at a position blocking the cysteine binding cavity entrance. By comparison, the other members of UE2s have a conformation similar to the mutant or have another residue that blocks the binding cavity. That can explain the NSC697923 specificity for UBE2N compared to the other member of UE2s.

Building on its *in vitro* selectivity, NSC697923 was later tested to improve the anti-tumor immune response and successfully inhibited melanoma growth *in vivo* in a mouse xenograft model, without any sign of toxicity or measurable weight loss.[19]

**UC-764864/65**

To identify a cysteine-reactive small-molecule inhibitor targeting UBE2N with clinical potential in acute myeloid leukemia (AML), Barreyro *et al.*[16,42] performed *in silico* structure-based screens of their in-house chemical library of 350,000 compounds. Leveraging the conjugated scaffolds of NSC697923 and BAY 11-7082 as a starting point, they docked 9,000 molecules to UBE2N. Subsequently the top 160 scoring compounds were evaluated for their inhibitory effect on MOLM-13 (human leukemia) cells using a cell proliferation assay.

The top 14 cytotoxic derivatives were then rescreened at lower concentrations. In parallel, UBE2N activity was evaluated in THP-1 human leukemia cell-line containing a reporter for NF-κB activation, hence evaluating UBE2N activity. Among them, 2 molecules (UC-764864 and UC-764865) have a cytotoxic effect and inhibit UBE2N-dependent signalling in leukemia cells.

MALDI TOF-MS analysis confirms the covalent binding mode of UC764864/65 to UBE2N. Incubation with the inhibitor resulted in a mass shift of approximately 160 Da in wild-type UBE2N protein, corresponding to the mass of the Michael addition adduct.

Using MALDI TOF-MS and CETSA assays, the authors also demonstrated that the two molecules did not react with mutant UBE2N (containing a Ser87 instead of a Cys87), its UBE2V1 co-factor lacking Cys87, or some closely related cysteine containing E2 conjugating enzymes (such as UBA1, UBE2T, PGD and GAPDH) suggesting that UC764864/65 are relatively selective for UBE2N in leukemia cells. In parallel, molecules were evaluated on normal cord blood CD34+ cells, where they displayed no cytotoxic activity.

An assessment of the drug-like properties of UC-764864 and UC-764865 showed that UC-764864 was readily metabolized in human and murine microsomes. UC-764865 presents better parameters, such as aqueous solubility, plasma stability and microsomal stability than UC-764864. Although not optimal, these values are compatible with animal model experimentation.

Next, to evaluate the *in vivo* antitumoral activity of UC-764865, the authors administrated the molecule to mice that have undergone an aggressive xenograft with cell line model of human AML. Interestingly, they registered a significant overall reduction of leukemic burden after treatment.

Building on these initial scaffolds, a hit to lead optimisation study is awaited to design UBE2N inhibitors with improved affinity, selectivity and overall better pharmacodynamic properties.

***Non-covalent UBE2N inhibitors***

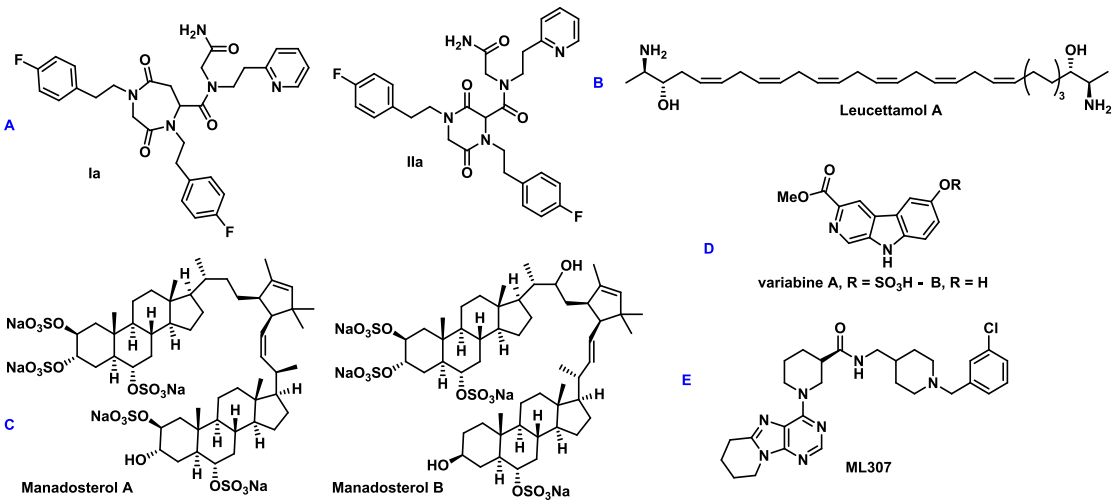


*Figure 7. Structures of non-covalent UBE2N inhibitors. A) Peptoid scaffolds. B) C) D) Natural molecules. E) Synthetic compound.*

The literature lists the following non-covalent inhibitors (figure 7): peptoid scaffolds, natural molecules and synthetic compounds. Unlike covalent inhibitors, the binding mode of non-covalent UBE2N inhibitors is not reported in the literature, and no crystallographic structures or NMR data on molecule/protein complexes have been described.

**Molecules of natural origin: Leucettamol, Manadosterols and Variabines**

The first discovered disruptor of UBE2N-UBE2V1 interaction was a natural compound extracted from the marine sponge *Leucetta microrhapis* and identified as leucettamol A using

spectroscopic analysis.[43] (figure 6. B.) Leucettamol A has an Inhibitory Concentration ($IC_{50}$) of approximately 50 µg/mL (106 µM) by ELISA. To investigate the SAR, two derivatives of leucettamol A (a hydrogenated and a tetraacetate) were synthesized and evaluated. The hydrogenated derivative displayed increased potency compared to leucettamol A, whereas the tetraacetate derivative was inactive. This suggests that the hydroxy and/or amino groups of leucettamol are crucial for the inhibitory activity. Instability and propensity for isomerization of Leucettamol A limit its potential as a drug candidate.

Therefore, Tsakumoto *et al.* extended this work using another species of sponge: *Lissodendryx fibrosa*,[44] and identified manadosterols, which also inhibit the UBE2N- UBE2V1 interaction in ELISA assay (figure 6. C.). Manadosterols A and B inhibited the UBE2N–UBE2V1 interaction with $IC_{50}$ values of 0.09 and 0.13 µM, respectively making them significantly more potent than leucettamol A. Notably, both manadosterols share a structural feature of two linked sulfonated sterol cores.

Pursuing their research, Tsukamoto *et al.* further reported the isolation of two new β-carboline alkaloids, variabines A and B, from the Indonesian marine sponge *Luffariella variabilis* (figure 6. D.).[45] The UBE2N/UBE2V1 interaction was inhibited by variabine B, as determined by ELISA with $IC_{50}$ values 4 µg/mL (16 µM), whereas variabine A, sulfonated derivative of variabine A had little effect, indicating that the inhibitory activities are lost by sulfonation. Moreover, variabine A showed no inhibition of E1 activity or the p53/HDM2 (E3).

No additional studies, particularly *in vivo* investigations and evaluations of druggability parameters, were conducted using these natural compounds.

**Peptoids**

Peptoids, a class of peptidomimetics, offer advantages for drug discovery due to their stability and cell permeability. Scheper *et al.* investigated the potential of peptoid scaffolds to develop anticancer drugs targeting the interaction between UBE2N and UBE2V1.[46,47] Peptoids are mimes of α-peptides in which the side chain is attached to the backbone amide nitrogen instead of the α-carbon.[48] They can adopt 3D-conformations similar to peptides, while being more resistant to the action of peptidases and having a better cellular permeability.[49]

Starting from a docking analysis of the interaction surface between UBE2N and UBE2V1, Scheper *et al.* selected 5120 compounds from a combinatorial chemical library of peptoids.

Then, to test the ability of peptoids to inhibit the interaction of UBE2N with UBE2V1, the authors used yeast two-hybrid assay. This assay allows to readily determine the specificity of the inhibitory activities on a fully defined protein-protein interaction and, simultaneously, constitutes a stringent filter for the bioavailability of active molecules.

Based on their data, they performed a molecular docking study and a virtual screening, allowing to highlight two cyclic compounds with the most favourable interactions with UBE2N.

The two compounds were subsequently synthesized and the affinity for UBE2N was confirmed by both yeast two-hybrid and SPR assays (figure 6. A.). The antitumoral activity of the hits were evaluated *in vivo* in a mouse xenograft model (PC-3 prostate cancer cells) and data showed a decrease in the tumor size and sensitization to doxorubicin. The two peptoids were shown to perturb the UBE2N/UBE2V1 interaction and inhibit NF-κB activation.

However, the selectivity towards other ubiquitin conjugating enzymes has not been evaluated and the use of these molecules in therapy remains limited because of the poor pharmacokinetic properties of peptoids.

### Synthetic molecule ML307

The most *in vitro* potent non-covalent inhibitor of UBE2N was reported by Ardecky *et al.* in 2010.[50] (figure 6.E.) Their aim was to develop small molecules inhibitors that binds UBE2N without forming covalent bond. They implemented a large-scale screening approach using the US National Institutes of Health (NIH) Molecular Libraries Program (MLP) collection containing around 350,000 compounds. The screening process involved a first TR-FRET based ubiquitination assay to select active compounds. To sort the results, a sulfhydryl (caspase 3) counterscreen was designed to confirm hits from the TR-FRET assay. The activities ($IC_{50}$) of the selected 1250 compounds were confirmed in ten-points dose response titration. Among the 72 members of the most potent scaffolds, several were excluded due to their frequent hitter or Michael acceptor properties. A molecule containing a 7,8,9,10-tetrahydro-6*H*-azepino[1,2-e]purine scaffold was identified among the most potent compounds and SAR studies were conducted in a hit-to-lead process. 77 compounds were synthesized to perform SAR studies, allowing identification of ML307 as the most promising molecule ($IC_{50}$ = 781 nM). While this potency is lower compared to some previously described natural inhibitors, the authors highlight that leucettamol A lacked detectable activity against UBE2N in their in-house screening assay (without mentioning the detail of their inhouse screening in that report).

An *in vitro* pharmacology screen of ML307 was conducted to afford preliminary ADME properties. ML307 is highly soluble in aqueous media at different pH and is stable in plasma. It exhibits also a good transcellular passage, evaluated by Parallel Artificial Membrane Permeability Assay (PAMPA), consistent with its estimated logP (AlogP=1.079). Unfortunately, ML307 has a poor microsomal stability, limiting its use in *in vivo* models and in a human therapeutic context.

In the future, additional SAR studies should be conducted to improve the pharmacokinetics properties of ML307. Although the toxicity on human hepatocytes was evaluated, more investigations on cellular models are also awaited to specify the mechanism of action of ML307. The selectivity of the molecule against other E2 ligases also need to be determined.

ML307 remains a useful *in vitro* tool for these fundamental biological studies, and further investigations on cellular model.

Furthermore, given that all screening results are publicly available, this open-access data can facilitate further SAR studies around unexploited scaffolds. By leveraging these data, researchers can promote the discovery of novel non-covalent UBE2N inhibitors with promising therapeutic potential.

## PERSPECTIVE: TOWARDS THE DESIGN OF NEW UBE2N INHIBITORS

The most advanced molecules in terms of development are the covalent inhibitors due to the wealth of available data, notably regarding their interaction mode with the target and having demonstrated *in vivo* efficacy in animal models, thereby underlining the interest to develop UBE2Ni.

The mechanism of action of these compounds involves the formation of a covalent bond with protein nucleophiles, mostly cysteines, which is relevant in the context of UBE2N inhibition. The electrophilic functional groups on covalent inhibitors are called “warheads”. Various warheads have been developed that can interact with cysteine, providing the key building blocks for covalent drugs to form covalent bond.[51] Advantages of using covalent drugs include a longer residence time and high binding affinity,[52] leading to a reduced risk for the

development of drug resistance: molecules can maintain high target engagements with limited plasma levels.[53] The main drawback remains the issue of target selectivity. Due to their highly reactive functions, covalent ligands non-selectively modify non-target protein, leading to potential off-target effects and toxicities.[54] For the development of future covalent inhibitors, the nature of the covalent-warhead is an interesting avenue to explore to improve the inhibitor selectivity.[55]

Computer-aided drug design is a tool of choice for guiding synthetic work to obtain new and more selective hits. Although the majority of docking methods development has been focused on the effective prediction of the binding modes of non-covalent inhibitors, nowadays, some software (i.e. Gold, DOCKovalent, and CovDock etc.) are emerging to perform docking studies of covalent inhibitors.[56,57] However, the implementation of molecular dynamics simulations remains challenging at present.[58,59]

To address the challenge of off-target effects associated with covalent inhibitors and to develop more selective molecules, researchers can explore the development of non-covalent inhibitors. Currently, there are few descriptions of potential non-covalent UBE2N inhibitors, but no studies have described the binding mechanisms of these molecules to their target.

Computer-aided drug design, especially docking studies, can be valuable to elucidate the binding site of non-covalent inhibitors on UBE2N. This information is crucial for the rational design of more potent and selective inhibitors in the future. Furthermore, fundamental cell biology studies are also essential to clarify the mechanism of action of both existing and future non-covalent UBE2N inhibitors. Understanding how these molecules affect cellular processes is critical to confirm their relevance as oncology therapeutics.

Given the strong structural analogy between the UBE2N partners (UBE2V2 and UBE2V1), the design of a selective protein-protein interaction disruptor seems compromised, especially as the differences between the two proteins are all outside of the interaction site with UBE2N. Despite this selectivity challenge, from a therapeutic perspective in the context of cancer, inhibiting both UBE2N interactions holds promise, because of the potential synergistic anti-cancer effect described above. However, high selectivity towards other E2 ligases should be a key consideration for the development of new therapeutic modalities.

UBE2N double KO has been shown to be embryonic lethal in mice,[60] raising questions about the potential side effects of UBE2N inhibition *in vivo*. However, a repeated administration (2 doses of 25 mg/kg per week during 2 weeks) of UC-764865 in healthy mice demonstrated that the treatment is well tolerated (not affecting body weight, hematologic parameters nor survival). Moreover, a histological evaluation of several tissues showed no evidence of overall tissue toxicity at the tested doses.[16] In addition, *in vivo* use of NSC697923 (5 mg/kg every other day during 10 days) in mice xenografted with melanoma tumour cells did not lead to any detectable toxicity.[19] Because murine and human UBE2N show a 100% homology, these *in vivo* data do support at this stage the further development of UBE2N inhibitors aiming for a use in humans.

The search for UBE2N inhibitors presents an exciting challenge for the scientific community. Several teams have developed screening tools, which are accessible to research programs. For example, Madiraju *et al*.[61] and Weber *et al*.[62] have proposed high-throughput screening assays strategies to identify new inhibitors, though they did not report to have performed them yet.

Lastly, it should not be forgotten that to obtain a drug candidate, an early assessment of the druggability of compounds is essential in a hit-to-lead approach.[63,64] While Table 1 presents a diverse array of UBE2N inhibitors, a critical challenge lies in their pharmacokinetic (ADME)

properties. From this pojnt of view, covalent hits seem compatible with the development of a potential drug candidate. However, calculators used are based on conventional inhibitors, which could limit the interpretation of these calculations. As mentioned above, covalent binding is achieved through nucleophilic activity of thiol cysteines. As a result, these compounds may be too reactive and fail to reach their site of action. This reactivity seems to be a limiting factor in the case of UC764865: the data predicting its microsomal stability are consistent with relative stability, whereas in the experiment, it turned out to be a rather unstable compound whose administration could not be transposable to humans. On the other hand, promising activity can be observed for non-covalent inhibitors, but their pharmacokinetic parameters are not compatible with more conventional drug design rules. Further work could be undertaken on these molecular scaffolds, using pharmacomodulation to obtain hits able to achieve good activity while exhibiting pharmacokinetic properties suitable for later development, particularly in terms of metabolic stability. Therefore, pharmacokinetics parameters will need to be taken into account as early as possible in the development of future UBE2N inhibitors if there is to eb any hope of their application in human therapy.

Targeting DNA repair is considered a relevant strategy for developing efficient molecules in cancer treatment. UBE2N could be a new target of interest in this regard, and UBE2N inhibitors would boost the arsenal of anticancer therapies targeting DNA repair. Literature data on existing compounds show encouraging results, although a number of challenges remain in terms of pharmacokinetics and compound selectivity for covalent inhibitors before these compounds enter the clinical evaluation phase. Very few UBE2Ni, in particular non covalent inhibitors have been reported in the literature, but recent advances in the scientific community on understanding of UBE2N, both on its structure and its functions in the cell, provide medicinal chemists with precious information for designing new classes of UBE2Ni.

*Table 1. Comparison of early ADME parameters, in vitro and in vivo evaluation of UBE2N inhibitors. Data available on literature were compared to ideal parameters according to Hughes et al.[63] When data was not found, each parameter was estimated using the suitable predictive web servers (i.e. Marvin Sketch, QikProp, PredMS, Swiss ADME, SuperCYPsPred, Vienna LiverTox, vNN-ADMET). Depending on the result, parameters were classed in three categories using a colour code (in green: ok – in orange – be careful- in red: not ok).*

| | | | Non-covalent hits | | Covalent hits | | |
|---|---|---|---|---|---|---|---|
| | | | **IA** | **ML307** | **BAY 11-7082** | **NSC697923** | **UC764865** |
| **Early ADME para-meters** | **Aqueous solubility** | **Measured (ideal >100 µM)*** | *Data not found* | 352 µM | *Data not found* | *Data not found* | 5mM |
| | | Estimated *(Marvin Sketch)* Log S / pH = 7.4 | -5 / 10 µM | - | - 2.83 / 1.48 mM | - 3.84 / 145 µM | - |
| | **Log $D_{7.4}$ // Log P** | **Measured (ideal 0–3)*** | *Data not found* | *Data not found* | *Data not found* | *Data not found* | *Data not found* |
| | | Estimated Log $D_{7.4}$ (*Marvin Sketch*) | 1.63 | 3.33 | 1.71 | 2.61 | 4.22 |
| | **Microsomal stability ($Cl_{int}$)** | **Measured (ideal < 30 mL.min$^{-1}$.mg$^{-1}$ proteins)*** | *Data not found* | 14% remain at 1 hour | *Data not found* | *Data not found* | 20 % remain at 1 hour |
| | | Estimated (*PredMS*) [65] [Stable > +50% at 30 min / Instable < 50% at 30 min] | Unstable | Unstable | Stable | Stable | Instable |
| | | Estimated *(QikProp MAESTRO)* (number of metabolites, good if <7) | 9 | 5 | 1 | 2 | 3 |
| | **CYP 450 inhibitor** | **Measured (ideal>10 mM)*** | *Data not found* | *Data not found* | *Data not found* | *Data not found* | *Data not found* |
| | | Estimated (*Swiss ADME / SuperCYPsPred*) | Yes/No | Yes/No | No/No | No/No | Yes/Yes |

| | | | | | | | |
|---|---|---|---|---|---|---|---|
| | **Caco-2 permeability $P_{app}$** | **Measured (ideal>1 x $10^{-6}$ $cm^{-1}$ (asymmetry <2) (= 10 nm))*** | *Data not found* | 776. $10^{-6}$ $cm.s^{-1}$ | *Data not found* | *Data not found* | *Data not found* |
| | | Estimated GI Absorption - *Swiss ADME* / $P_{app}$ nm/*s QikProp MAESTRO* / % human oral absorption *QikProp MAESTRO* | High/40/53% | High/231/ 83% | High/390/ 76% | High/167/72 % | High/1568/ 100% |
| | **MDR1-MDCK permeability** | **Measured (ideal>10 x $10^{-6}$ $cm^{-1}$ (asymmetry <2) (= 100 nm))*** | *Data not found* | *Data not found* | *Data not found* | *Data not found* | *Data not found* |
| | | Estimated P-gp Substrat (*Swiss ADME*) / P-gp Inhibition // Transport (*Vienna LiverTox*)[66] | Yes/yes//yes | Yes/yes// yes | No/no//no | No/no//no | No/no//no |
| | **HepG2 hepatotoxicity** | **Measured (ideal: no effect at 50 x $IC_{50}$ or $EC_{50}$)*** | *Data not found* | *Data not found* | *Data not found* | *Data not found* | No effect |
| | | Drug-Induced liver injury (*Vienna LiverTox*)[66] | Yes | Yes | Yes | Yes | Yes |
| | **Cytotoxicity in suitable cell** | **Measured (ideal: no effect at 50 x $IC_{50}$ or $EC_{50}$)*** | *Data not found* | LC50 > 50 µM *(on hepatocyte cell lines)* | *Data not found* | *Data not found* | $DL_{50}$ [2-3] µM Ok on MOLM-13 and MDSL cell lines |
| | | Estimated Cytotoxicity (*vNN-ADMET*)[67] | No | No | No | No | No |
| ***Activity*** | ***In vitro* activity ($IC_{50}$)** | | 10 pM | 781 nM | 10 µM (ICAM-1 and E-selectin) | 1,737 µM (caspase 1 inhibition) | 0,14 µM |
| | ***In vivo* activity** | | Xenograft Mice-PC-3 prostate cancer cells decrease of the tumor size and sensitization to doxorubicin | No | No | Induce cell death on human neuroblastoma xenografts in an orthotopic mouse model | Mice-AML Antitumoral activity but not sufficient as a single agent |

* according to Hughes *et al.*[63]

## AUTHOR INFORMATIONS

### Corresponding Authors

Charline Kieffer charline.kieffer@unicaen.fr and Matthieu Meryet-Figuière m.meryet-figuiere@baclesse.unicancer.fr

### Author contributions

C.G. and J.S.S. performed chemoinformatic analysis, J.S.S., C.G., C.K., F.S., M.M.F. and L.B.W. wrote the manuscript, F.S. and C. G. prepared figures, L.I., S.U.K. and A.S.V. contributed to reviewing the manuscript.

### Notes

The authors declare no competing financial interest.

### Biographies

**Côme Ghadi** obtained his master's degree in In Silico Drug Design from Université Paris Cité in 2022. Subsequently, he was recruited as a Research Engineer at the Centre d'Etudes et de Recherche sur le Médicament de Normandie (CERMN) at the University of Caen Normandy (France), under the supervision of Professor Jana Sopkova-de Oliveira Santos. His research focused on the discovery of a new non-covalent inhibitor of UBE2N.The inhibition of UBE2N aims to enhance the effectiveness of PARP inhibitors, which have shown

promise in the treatment of ovarian cancer. Since 2023, he has been a PhD student in the same laboratory. His current work focuses on resensitizing antibiotics through the discovery of new DltB inhibitors.

**Matthieu Meryet-Figuiere** obtained his PhD in Pharmacology from Caen University, France, in 2010. He was then a post-doctoral researcher in Chandra Kanduri group in Göteborg University, Sweden, until 2014. He is currently researcher at the Comprehensive Cancer Center François Baclesse in Caen. He has been mainly focused on the roles and functions of short and long non-coding RNAs in the response to treatments of ovarian cancers. This research recently led him to study the involvement of DNA repair mechanisms and their alterations in ovarian cancer, where he could identify UBE2N as a promising target in this disease. His research goals are aimed to identify how modulating DNA repair mechanisms could help develop innovative therapeutic strategies to improve the care of ovarian cancer patients.

**Léonie Ibazizene** obtained his master degree in 2023 from the University of Caen Normandie, France. Currently, she is PhD student at INSERM U1086 ANTICIPE in France. Her ongoing project focuses on the validation of UBE2N as therapeutic target in ovarian cancers and the development of UBE2N inhibitors to sensitize to PARP inhibitors.

**Charline Kieffer** graduated from the University of Aix Marseille with both a PharmD (2014) and a PhD in Medicinal Chemistry (2014). After several industrial and academic postdoctoral fellowships, she was recruited to the University of Caen Normandie in 2017 as Associate Professor in Medicinal Chemistry. Her expertise area includes drug design of small molecules, especially fragment-based drug design and structure-based drug design. She is more particularly involved in the synthesis of small molecules that disrupt protein-protein interactions, with applications in oncology, inflammation and infectiology.

**Florian Schwalen** graduated with a Master's degree in Drug Design at the University of Caen in 2022 and a Master's degree in Pharmaceutical Science at the University of Toulouse in 2020. He is pursuing his Master's degree as a PhD candidate in Caen University in the research group of Prof. AS Voisin Chiret and as PharmD candidate at Caen University Hospital. His research focuses on the design and synthesis of small molecules with anti-cancer activity.

**Jana Sopková-de Oliveira Santos** obtained her "Rerum Naturalium Doctoris" (1989) in Chemical Physics from Charles University of Prague (Czech Republic) and her Ph.D. (1994) from University of Paris XI (France) as well as from Charles University of Prague (1994). She then worked on various postdoctoral research projects involving structural studies (X-ray crystallography, modelling) and spectroscopic studies of proteins (IOCB of Czech Academy of Sciences, laboratory LBPM of CEA Saclay and French synchrotron LURE - Orsay). Since 1999, Jana has been an Assistant Professor and now Professor of general chemistry and biophysics at University of Caen Normandy. Her research interests include X-ray diffraction studies of small organic compounds and molecular modeling approaches, especially dynamics simulations.

**Shafi Ullah Khan** obtained his Ph.D. in Medicinal Chemistry from Monash University in 2021. During his PhD, he worked on the identification of potential modulators of G protein-coupled estrogen receptor-1 (GPER-1) as a potential therapy in breast cancer resistance. Following the completion of his Ph.D., he served as a faculty member at ABASYN University, Pakistan, from 2021 to 2022. Subsequently, in 2022, he transitioned to the industry, holding the position of R&D Manager at QARSHI Brands, Pakistan, until 2023. Currently, he is a Marie Skłodowska-Curie-Cofund Postdoctoral Fellow at INSERM U1086 ANTICIPE in

France. His ongoing project focuses on developing novel, non-covalent UBE2N inhibitors to enhance ovarian cancer treatment. These inhibitors aim to sensitize ovarian cancer cells to PARP inhibitors, potentially leading to more effective therapies.

**Anne Sophie Voisin-Chiret** holds her PharmD (2002) and a PhD from the University of Caen (2005), and after completing a postdoctoral period, she was appointed Lecturer in Medicinal Chemistry in the School of Pharmacy at the University of Caen (2007). Since September 2015, she has assumed the position of Prof of Medicinal Chemistry. Her research interests include medicinal chemistry in the field of protein-protein interactions, in order to design oligo(het)aromatic compounds that mimic proteins to fold into well-defined conformations, such as helices and β-sheets. Currently she is leading a research project dedicated to the study of the challenging class of protein-protein interfaces in order to design drug-like modulators of protein-protein interactions particularly in oncology and neurodegenerative diseases.

**Louis-Bastien Weiswald** obtained his Ph.D. degree in biological sciences in 2010 from University of Pierre and Marie Curie in Paris. He completed postdoctoral fellowships at Curie Institute and then at British Columbia Cancer Agency before returning to France in 2017. He is currently principal investigator at Comprehensive Cancer Center François Baclesse and co-head of the patient-derived tumor organoid core facility ORGAPRED. His career has focused so far on the development of innovative anticancer therapies and associated predictive tools (biomarkers, functional assays) enabling the selection of patients likely to benefit from these strategies. His current research interests focus on improving management of ovarian cancer through the development of new therapeutic strategies targeting DNA repair and the implementation of predictive functional assay based on patient-tumor organoids.

**ACKNOWLEDGMENTS:**

This project has received funding from the European Union's Horizon 2020 research and innovation programme under the Marie Skłodowska-Curie grant agreement No 101034329. Shafi Ullah Khan is the Recipient of the WINNINGNormandy Program supported by the Normandy Region. Florian Schwalen thanks ARS Normandie for financial support. This work was supported by the 'Ligue Contre le Cancer' (Normandy confederation, to Louis-Bastien Weiswald). Léonie Ibazizène is the recipient of a doctoral fellowship from the Normandy Region. This work was supported by the Cancéropôle Nord-Ouest (grant to Louis-Bastien Weiswald), and Inserm (grant Aviesan/ITMO Cancer to Matthieu Meryet-Figuiere).

**ABBREVIATIONS USED:**

ADME, absorption, distribution, metabolism, excretion; AML, acute myeloid leukemia; ATM, ataxia-telangiectasia mutated; ATR, ataxia telangiectasia and Rad3 related gene; BRCA, breast cancer gene; CETSA, cellular thermal shift assay; CHEK2, checkpoint kinase 2; CYP 450, cytochrome P450; DLBCL, diffuse large B-cell lymphoma; DNA, deoxyribonucleic acid; $EC_{50}$, half maximal effective concentration; ELISA, enzyme-linked immunosorbent assay; FDA, food and drug administration; GAPDH, glyceraldehyde-3-phosphate dehydrogenase; HDM2, mouse double minute 2 proto-oncogene; HR, homologous recombination; HRD, homologous recombination deficiency; $IC_{50}$, half maximal inhibitory concentration; IKK, IκB kinase; ISG, interferon-stimulated gene; LNX1, ligand of numb-protein X 1; MALDI TOF-MS, matrix assisted laser desorption ionization-time of flight mass spectrometry; MDR1-MDCK, multidrug resistance gene-1-madin-darby canine kidney cells; MLP, molecular libraries program; NF-κB, nuclear factor kappa-light-chain-enhancer of activated B cells; NHEJ, non-

homologous end joining; NIH, national institutes of health; OPSL1, protein octopus-like 1; OTUB1, ubiquitin aldehyde binding 1; PALB2, partner and localizer of BRCA2; PAMPA, parallel artificial membrane permeability assay; PARP, poly (ADP-ribose) polymerase; PARPi, poly (ADP-ribose) polymerase inhibitors; PDB, protein data bank; PD-L1, programmed death-ligand 1; PGD, phosphogluconate dehydrogenase; P-gp, permeability-glycoprotein; RAP80, receptor-associated protein 80; RNF, ring finger protein; SAR, structure-activity relationship; SPR, surface plasmon resonance; STIP1, stress induced phosphoprotein 1; SUMO, small ubiquitin-like modifier; TNF, tumor necrosis factor; TRAF6, TNF receptor associated factor 6; TR-FRET, time-resolved fluorescence energy transfer; TRIM, tripartite motif containing; Ub, ubiquitin; UBA1, ubiquitin like modifier activating enzyme 1; UBE2N, ubiquitin-conjugating enzyme E2 N; UBEN2i, ubiquitin-conjugating enzyme E2 N inhibitor; UBE2V1, ubiquitin conjugating enzyme E2 V1; UBE2V2, ubiquitin conjugating enzyme E2 V2; UE2, small ubiquitin-like modifier; ubiquitin-converting enzyme 2; ZNRF1, zinc and ring finger 1

## REFERENCES:


(1) Sheng, Y.; Hong, J. H.; Doherty, R.; Srikumar, T.; Shloush, J.; Avvakumov, G. V.; Walker, J. R.; Xue, S.; Neculai, D.; Wan, J. W.; Kim, S. K.; Arrowsmith, C. H.; Raught, B.; Dhe-Paganon, S. A Human Ubiquitin Conjugating Enzyme (E2)-HECT E3 Ligase Structure-Function Screen. *Mol Cell Proteomics* **2012**, *11* (8), 329–341.

(2) Sievers, F.; Wilm, A.; Dineen, D.; Gibson, T. J.; Karplus, K.; Li, W.; Lopez, R.; McWilliam, H.; Remmert, M.; Söding, J.; Thompson, J. D.; Higgins, D. G. Fast, Scalable Generation of High-Quality Protein Multiple Sequence Alignments Using Clustal Omega. *Mol Syst Biol* **2011**, *7*, 539.

(3) Stewart, M. D.; Ritterhoff, T.; Klevit, R. E.; Brzovic, P. S. E2 Enzymes: More than Just Middle Men. *Cell Res* **2016**, *26* (4), 423–440.

(4) Du, X.; Song, H.; Shen, N.; Hua, R.; Yang, G. The Molecular Basis of Ubiquitin-Conjugating Enzymes (E2s) as a Potential Target for Cancer Therapy. *Int J Mol Sci* **2021**, *22* (7), 3440.

(5) Garg, P.; Ceccarelli, D. F.; Keszei, A. F. A.; Kurinov, I.; Sicheri, F.; Sidhu, S. S. Structural and Functional Analysis of Ubiquitin-Based Inhibitors That Target the Backsides of E2 Enzymes. *J Mol Biol* **2020**, *432* (4), 952–966.

(6) Bui, Q. T.; Hong, J. H.; Kwak, M.; Lee, J. Y.; Lee, P. C.-W. Ubiquitin-Conjugating Enzymes in Cancer. *Cells* **2021**, *10* (6), 1383.

(7) Hofmann, R. M.; Pickart, C. M. Noncanonical MMS2-Encoded Ubiquitin-Conjugating Enzyme Functions in Assembly of Novel Polyubiquitin Chains for DNA Repair. *Cell* **1999**, *96* (5), 645–653.

(8) Zhang, Y.; Li, Y.; Yang, X.; Wang, J.; Wang, R.; Qian, X.; Zhang, W.; Xiao, W. Uev1A-Ubc13 Catalyzes K63-Linked Ubiquitination of RHBDF2 to Promote TACE Maturation. *Cell Signal* **2018**, *42*, 155–164.

(9) Iwai, K. Diverse Ubiquitin Signaling in NF-κB Activation. *Trends Cell Biol* **2012**, *22* (7), 355–364.

(10) Ikeda, F.; Dikic, I. Atypical Ubiquitin Chains: New Molecular Signals. “Protein Modifications: Beyond the Usual Suspects” Review Series. *EMBO Rep* **2008**, *9* (6), 536–542.

(11) Komander, D.; Rape, M. The Ubiquitin Code. *Annu Rev Biochem* **2012**, *81*, 203–229.

(12) Panier, S.; Durocher, D. Regulatory Ubiquitylation in Response to DNA Double-Strand Breaks. *DNA Repair (Amst)* **2009**, *8* (4), 436–443.

(13) Ye, Y.; Rape, M. Building Ubiquitin Chains: E2 Enzymes at Work. *Nat Rev Mol Cell Biol* **2009**, *10* (11), 755–764.

(14) Zhang, C.; Jia, Q.; Zhu, L.; Hou, J.; Wang, X.; Li, D.; Zhang, J.; Zhang, Y.; Yang, S.; Tu, Z.; Yan, X.-X.; Yang, W.; Li, S.; Li, X.-J.; Yin, P. Suppressing UBE2N Ameliorates

Alzheimer's Disease Pathology through the Clearance of Amyloid Beta. *Alzheimers Dement* **2024**.
(15) Zhao, G. Y.; Sonoda, E.; Barber, L. J.; Oka, H.; Murakawa, Y.; Yamada, K.; Ikura, T.; Wang, X.; Kobayashi, M.; Yamamoto, K.; Boulton, S. J.; Takeda, S. A Critical Role for the Ubiquitin-Conjugating Enzyme Ubc13 in Initiating Homologous Recombination. *Mol Cell* **2007**, *25* (5), 663–675.
(16) Barreyro, L.; Sampson, A. M.; Ishikawa, C.; Hueneman, K. M.; Choi, K.; Pujato, M. A.; Chutipongtanate, S.; Wyder, M.; Haffey, W. D.; O'Brien, E.; Wunderlich, M.; Ramesh, V.; Kolb, E. M.; Meydan, C.; Neelamraju, Y.; Bolanos, L. C.; Christie, S.; Smith, M. A.; Niederkorn, M.; Muto, T.; Kesari, S.; Garrett-Bakelman, F. E.; Bartholdy, B.; Will, B.; Weirauch, M. T.; Mulloy, J. C.; Gul, Z.; Medlin, S.; Kovall, R. A.; Melnick, A. M.; Perentesis, J. P.; Greis, K. D.; Nurmemmedov, E.; Seibel, W. L.; Starczynowski, D. T. Blocking UBE2N Abrogates Oncogenic Immune Signaling in Acute Myeloid Leukemia. *Sci Transl Med* **2022**, *14* (635).
(17) Antonangeli, F.; Natalini, A.; Garassino, M. C.; Sica, A.; Santoni, A.; Di Rosa, F. Regulation of PD-L1 Expression by NF-κB in Cancer. *Front Immunol* **2020**, *11*, 584626.
(18) Zou, R.; Xu, H.; Li, F.; Wang, S.; Zhu, L. Increased Expression of UBE2T Predicting Poor Survival of Epithelial Ovarian Cancer: Based on Comprehensive Analysis of UBE2s, Clinical Samples, and the GEO Database. *DNA Cell Biol* **2021**, *40* (1), 36–60.
(19) Dikshit, A.; Jin, Y. J.; Degan, S.; Hwang, J.; Foster, M. W.; Li, C.-Y.; Zhang, J. Y. UBE2N Promotes Melanoma Growth via MEK/FRA1/SOX10 Signaling. *Cancer Res* **2018**, *78* (22), 6462–6472.
(20) Pulvino, M.; Liang, Y.; Oleksyn, D.; DeRan, M.; Van Pelt, E.; Shapiro, J.; Sanz, I.; Chen, L.; Zhao, J. Inhibition of Proliferation and Survival of Diffuse Large B-Cell Lymphoma Cells by a Small-Molecule Inhibitor of the Ubiquitin-Conjugating Enzyme Ubc13-Uev1A. *Blood* **2012**, *120* (8), 1668–1677.
(21) Rubio, N.; Villacampa, M. M.; Blanco, J. Traffic to Lymph Nodes of PC-3 Prostate Tumor Cells in Nude Mice Visualized Using the Luciferase Gene as a Tumor Cell Marker. *Lab Invest* **1998**, *78* (10), 1315–1325.
(22) Wambecke, A.; Ahmad, M.; Morice, P.; Lambert, B.; Weiswald, L.; Vernon, M.; Vigneron, N.; Abeilard, E.; Brotin, E.; Figeac, M.; Gauduchon, P.; Poulain, L.; Denoyelle, C.; Meryet-Figuiere, M. The lncRNA 'UCA1' Modulates the Response to Chemotherapy of Ovarian Cancer through Direct Binding to miR-27a-5p and Control of UBE2N Levels. *Mol Oncol* **2021**, *15* (12), 3659–3678.
(23) Zhang, P.; Wang, L.; Rodriguez-Aguayo, C.; Yuan, Y.; Debeb, B. G.; Chen, D.; Sun, Y.; You, M. J.; Liu, Y.; Dean, D. C.; Woodward, W. A.; Liang, H.; Yang, X.; Lopez-Berestein, G.; Sood, A. K.; Hu, Y.; Ang, K. K.; Chen, J.; Ma, L. miR-205 Acts as a Tumour Radiosensitizer by Targeting ZEB1 and Ubc13. *Nat Commun* **2014**, *5*, 5671.
(24) Yin, P.; Tu, Z.; Yin, A.; Zhao, T.; Yan, S.; Guo, X.; Chang, R.; Zhang, L.; Hong, Y.; Huang, X.; Zhou, J.; Wang, Y.; Li, S.; Li, X.-J. Aged Monkey Brains Reveal the Role of Ubiquitin-Conjugating Enzyme UBE2N in the Synaptosomal Accumulation of Mutant Huntingtin. *Hum Mol Genet* **2015**, *24* (5), 1350–1362.
(25) Szklarczyk, D.; Santos, A.; von Mering, C.; Jensen, L. J.; Bork, P.; Kuhn, M. STITCH 5: Augmenting Protein-Chemical Interaction Networks with Tissue and Affinity Data. *Nucleic Acids Res* **2016**, *44* (D1), D380-384.
(26) Altschul, S. F.; Gish, W.; Miller, W.; Myers, E. W.; Lipman, D. J. Basic Local Alignment Search Tool. *J Mol Biol* **1990**, *215* (3), 403–410.
(27) Hussein, H. A.; Borrel, A.; Geneix, C.; Petitjean, M.; Regad, L.; Camproux, A.-C. PockDrug-Server: A New Web Server for Predicting Pocket Druggability on Holo and Apo Proteins. *Nucleic Acids Res* **2015**, *43* (W1), W436-442.
(28) Sato, Y.; Yamagata, A.; Goto-Ito, S.; Kubota, K.; Miyamoto, R.; Nakada, S.; Fukai, S. Molecular Basis of Lys-63-Linked Polyubiquitination Inhibition by the Interaction between Human Deubiquitinating Enzyme OTUB1 and Ubiquitin-Conjugating Enzyme UBC13. *J Biol Chem* **2012**, *287* (31), 25860–25868.

(29) Wiener, R.; Zhang, X.; Wang, T.; Wolberger, C. The Mechanism of OTUB1-Mediated Inhibition of Ubiquitination. *Nature* **2012**, *483* (7391), 618–622.
(30) Hodge, C. D.; Edwards, R. A.; Markin, C. J.; McDonald, D.; Pulvino, M.; Huen, M. S. Y.; Zhao, J.; Spyracopoulos, L.; Hendzel, M. J.; Glover, J. N. M. Covalent Inhibition of Ubc13 Affects Ubiquitin Signaling and Reveals Active Site Elements Important for Targeting. *ACS Chem Biol* **2015**, *10* (7), 1718–1728.
(31) Pierce, J. W.; Schoenleber, R.; Jesmok, G.; Best, J.; Moore, S. A.; Collins, T.; Gerritsen, M. E. Novel Inhibitors of Cytokine-Induced IkappaBalpha Phosphorylation and Endothelial Cell Adhesion Molecule Expression Show Anti-Inflammatory Effects in Vivo. *J Biol Chem* **1997**, *272* (34), 21096–21103.
(32) Lee, J.; Rhee, M. H.; Kim, E.; Cho, J. Y. BAY 11-7082 Is a Broad-Spectrum Inhibitor with Anti-Inflammatory Activity against Multiple Targets. *Mediators Inflamm* **2012**, *2012*, 416036.
(33) Juliana, C.; Fernandes-Alnemri, T.; Wu, J.; Datta, P.; Solorzano, L.; Yu, J.-W.; Meng, R.; Quong, A. A.; Latz, E.; Scott, C. P.; Alnemri, E. S. Anti-Inflammatory Compounds Parthenolide and Bay 11-7082 Are Direct Inhibitors of the Inflammasome. *J Biol Chem* **2010**, *285* (13), 9792–9802.
(34) Lee, H.-S.; Kim, S. D.; Lee, W. M.; Endale, M.; Kamruzzaman, S. M.; Oh, W. J.; Cho, J. Y.; Kim, S. K.; Cho, H.-J.; Park, H.-J.; Rhee, M. H. A Noble Function of BAY 11-7082: Inhibition of Platelet Aggregation Mediated by an Elevated cAMP-Induced VASP, and Decreased ERK2/JNK1 Phosphorylations. *Eur J Pharmacol* **2010**, *627* (1–3), 85–91.
(35) Coles, V. E.; Darveau, P.; Zhang, X.; Harvey, H.; Henriksbo, B. D.; Yang, A.; Schertzer, J. D.; Magolan, J.; Burrows, L. L. Exploration of BAY 11-7082 as a Potential Antibiotic. *ACS Infect Dis* **2022**, *8* (1), 170–182.
(36) Strickson, S.; Campbell, D. G.; Emmerich, C. H.; Knebel, A.; Plater, L.; Ritorto, M. S.; Shpiro, N.; Cohen, P. The Anti-Inflammatory Drug BAY 11-7082 Suppresses the MyD88-Dependent Signalling Network by Targeting the Ubiquitin System. *Biochem J* **2013**, *451* (3), 427–437.
(37) Krishnan, N.; Bencze, G.; Cohen, P.; Tonks, N. K. The Anti-Inflammatory Compound BAY 11-7082 Is a Potent Inhibitor of Protein Tyrosine Phosphatases. *FEBS J* **2013**, *280* (12), 2830–2841.
(38) Ghashghaeinia, M.; Giustarini, D.; Koralkova, P.; Köberle, M.; Alzoubi, K.; Bissinger, R.; Hosseinzadeh, Z.; Dreischer, P.; Bernhardt, I.; Lang, F.; Toulany, M.; Wieder, T.; Mojzikova, R.; Rossi, R.; Mrowietz, U. Pharmacological Targeting of Glucose-6-Phosphate Dehydrogenase in Human Erythrocytes by Bay 11–7082, Parthenolide and Dimethyl Fumarate. *Sci Rep* **2016**, *6*, 28754.
(39) Scaife, C. L.; Kuang, J.; Wills, J. C.; Trowbridge, D. B.; Gray, P.; Manning, B. M.; Eichwald, E. J.; Daynes, R. A.; Kuwada, S. K. Nuclear Factor kappaB Inhibitors Induce Adhesion-Dependent Colon Cancer Apoptosis: Implications for Metastasis. *Cancer Res* **2002**, *62* (23), 6870–6878.
(40) Chen, L.; Ruan, Y.; Wang, X.; Min, L.; Shen, Z.; Sun, Y.; Qin, X. BAY 11-7082, a Nuclear Factor-κB Inhibitor, Induces Apoptosis and S Phase Arrest in Gastric Cancer Cells. *J Gastroenterol* **2014**, *49* (5), 864–874.
(41) Kim, K.; Ryu, K.; Ko, Y.; Park, C. Effects of Nuclear Factor-kappaB Inhibitors and Its Implication on Natural Killer T-Cell Lymphoma Cells. *Br J Haematol* **2005**, *131* (1), 59–66.
(42) Starczynowski, D.; Barreyro, L.; Seibel, W. Rational Therapeutic Targeting of Oncogenic Immune Signaling States in Myeloid Malignancies via the Ubiquitin Conjugating Enzyme UBE2N. WO2020252487A1, December 17, **2020**.
(43) Tsukamoto, S.; Takeuchi, T.; Rotinsulu, H.; Mangindaan, R. E. P.; van Soest, R. W. M.; Ukai, K.; Kobayashi, H.; Namikoshi, M.; Ohta, T.; Yokosawa, H. Leucettamol A: A New Inhibitor of Ubc13-Uev1A Interaction Isolated from a Marine Sponge, Leucetta Aff. Microrhaphis. *Bioorg Med Chem Lett* **2008**, *18* (24), 6319–6320.
(44) Ushiyama, S.; Umaoka, H.; Kato, H.; Suwa, Y.; Morioka, H.; Rotinsulu, H.; Losung, F.; Mangindaan, R. E. P.; de Voogd, N. J.; Yokosawa, H.; Tsukamoto, S. Manadosterols A

and B, Sulfonated Sterol Dimers Inhibiting the Ubc13-Uev1A Interaction, Isolated from the Marine Sponge Lissodendryx Fibrosa. *J Nat Prod* **2012**, *75* (8), 1495–1499.
(45) Sakai, E.; Kato, H.; Rotinsulu, H.; Losung, F.; Mangindaan, R. E. P.; de Voogd, N. J.; Yokosawa, H.; Tsukamoto, S. Variabines A and B: New β-Carboline Alkaloids from the Marine Sponge Luffariella Variabilis. *J Nat Med* **2014**, *68* (1), 215–219.
(46) Scheper, J.; Guerra-Rebollo, M.; Sanclimens, G.; Moure, A.; Masip, I.; González-Ruiz, D.; Rubio, N.; Crosas, B.; Meca-Cortés, Ó.; Loukili, N.; Plans, V.; Morreale, A.; Blanco, J.; Ortiz, A. R.; Messeguer, À.; Thomson, T. M. Protein-Protein Interaction Antagonists as Novel Inhibitors of Non-Canonical Polyubiquitylation. *PLoS One* **2010**, *5* (6), e11403.
(47) Okatsu, T. T.; Sigmund, J. S.; Peypoch, Á. M.; Ortiz, Á. R.; Sanclimens, G.; Masip, I. M.; Fernandez, A. M.; González-Ruiz, D.; Morreale, A. Compound That Can Inhibit Ubc13-Uev Interactions, Pharmaceutical Compositions and Therapeutic Uses. EP2045251A1, April 8, **2009**.
(48) Fowler, S. A.; Blackwell, H. E. Structure-Function Relationships in Peptoids: Recent Advances toward Deciphering the Structural Requirements for Biological Function. *Org Biomol Chem* **2009**, *7* (8), 1508–1524.
(49) Tan, N. C.; Yu, P.; Kwon, Y.-U.; Kodadek, T. High-Throughput Evaluation of Relative Cell Permeability between Peptoids and Peptides. *Bioorg Med Chem* **2008**, *16* (11), 5853–5861.
(50) Ardecky, R.; Madiraju, C.; Matsuzawa, S.; Zou, J.; Ganji, S.; Pass, I.; Ngo, T. A.; Pinkerton, A. B.; Sergienko, E.; Su, Y.; Stonich, D.; Mangravita-Novo, A.; Vicchiarelli, M.; McAnally, D.; Smith, L. H.; Diwan, J.; Chung, T. D. Y.; Matsuzawa, Y.; Wimer, C.; Diaz, P. W.; Reed, J. C. Selective UBC 13 Inhibitors. In *Probe Reports from the NIH Molecular Libraries Program*; National Center for Biotechnology Information (US): Bethesda (MD), **2010**.
(51) Huang, F.; Han, X.; Xiao, X.; Zhou, J. Covalent Warheads Targeting Cysteine Residue: The Promising Approach in Drug Development. *Molecules* **2022**, *27* (22), 7728.
(52) Cheng, S.-S.; Yang, G.-J.; Wang, W.; Leung, C.-H.; Ma, D.-L. The Design and Development of Covalent Protein-Protein Interaction Inhibitors for Cancer Treatment. *J Hematol Oncol* **2020**, *13* (1), 26.
(53) Engel, J.; Richters, A.; Getlik, M.; Tomassi, S.; Keul, M.; Termathe, M.; Lategahn, J.; Becker, C.; Mayer-Wrangowski, S.; Grütter, C.; Uhlenbrock, N.; Krüll, J.; Schaumann, N.; Eppmann, S.; Kibies, P.; Hoffgaard, F.; Heil, J.; Menninger, S.; Ortiz-Cuaran, S.; Heuckmann, J. M.; Tinnefeld, V.; Zahedi, R. P.; Sos, M. L.; Schultz-Fademrecht, C.; Thomas, R. K.; Kast, S. M.; Rauh, D. Targeting Drug Resistance in EGFR with Covalent Inhibitors: A Structure-Based Design Approach. *J Med Chem* **2015**, *58* (17), 6844–6863.
(54) Sutanto, F.; Konstantinidou, M.; Dömling, A. Covalent Inhibitors: A Rational Approach to Drug Discovery. *RSC Med Chem* **2020**, *11* (8), 876–884.
(55) Baillie, T. A. Approaches to Mitigate the Risk of Serious Adverse Reactions in Covalent Drug Design. *Expert Opin Drug Discov* **2021**, *16* (3), 275–287.
(56) Kumalo, H. M.; Bhakat, S.; Soliman, M. E. S. Theory and Applications of Covalent Docking in Drug Discovery: Merits and Pitfalls. *Molecules* **2015**, *20* (2), 1984–2000.
(57) Boike, L.; Henning, N. J.; Nomura, D. K. Advances in Covalent Drug Discovery. *Nat Rev Drug Discov* **2022**, *21* (12), 881–898.
(58) Khan, S.; Bjij, I.; Olotu, F. A.; Agoni, C.; Adeniji, E.; S Soliman, M. E. Covalent Simulations of Covalent/Irreversible Enzyme Inhibition in Drug Discovery: A Reliable Technical Protocol. *Future Med Chem* **2018**, *10* (19), 2265–2275.
(59) Oyedele, A.-Q. K.; Ogunlana, A. T.; Boyenle, I. D.; Adeyemi, A. O.; Rita, T. O.; Adelusi, T. I.; Abdul-Hammed, M.; Elegbeleye, O. E.; Odunitan, T. T. Docking Covalent Targets for Drug Discovery: Stimulating the Computer-Aided Drug Design Community of Possible Pitfalls and Erroneous Practices. *Mol Divers* **2023**, *27* (4), 1879–1903.
(60) Joo, E.; Fukushima, T.; Harada, N.; Reed, J. C.; Matsuzawa, S.-I.; Inagaki, N. Ubc13 Haploinsufficiency Protects against Age-Related Insulin Resistance and High-Fat Diet-Induced Obesity. *Sci Rep* **2016**, *6*, 35983.

(61) Madiraju, C.; Welsh, K.; Cuddy, M. P.; Godoi, P. H.; Pass, I.; Ngo, T.; Vasile, S.; Sergienko, E. A.; Diaz, P.; Matsuzawa, S.-I.; Reed, J. C. TR-FRET-Based High-Throughput Screening Assay for Identification of UBC13 Inhibitors. *J Biomol Screen* **2012**, *17* (2), 163–176.
(62) Weber, E.; Rothenaigner, I.; Brandner, S.; Hadian, K.; Schorpp, K. A High-Throughput Screening Strategy for Development of RNF8-Ubc13 Protein-Protein Interaction Inhibitors. *SLAS Discov* **2017**, *22* (3), 316–323.
(63) Hughes, J.; Rees, S.; Kalindjian, S.; Philpott, K. Principles of Early Drug Discovery. *Br J Pharmacol* **2011**, *162* (6), 1239–1249.
(64) Strovel, J.; Sittampalam, S.; Coussens, N. P.; Hughes, M.; Inglese, J.; Kurtz, A.; Andalibi, A.; Patton, L.; Austin, C.; Baltezor, M.; Beckloff, M.; Weingarten, M.; Weir, S. Early Drug Discovery and Development Guidelines: For Academic Researchers, Collaborators, and Start-up Companies. In *Assay Guidance Manual*; Markossian, S., Grossman, A., Brimacombe, K., Arkin, M., Auld, D., Austin, C., Baell, J., Chung, T. D. Y., Coussens, N. P., Dahlin, J. L., Devanarayan, V., Foley, T. L., Glicksman, M., Gorshkov, K., Haas, J. V., Hall, M. D., Hoare, S., Inglese, J., Iversen, P. W., Kales, S. C., Lal-Nag, M., Li, Z., McGee, J., McManus, O., Riss, T., Saradjian, P., Sittampalam, G. S., Tarselli, M., Trask, O. J., Wang, Y., Weidner, J. R., Wildey, M. J., Wilson, K., Xia, M., Xu, X., Eds.; Eli Lilly & Company and the National Center for Advancing Translational Sciences: Bethesda (MD), **2004**.
(65) Ryu, J. Y.; Lee, J. H.; Lee, B. H.; Song, J. S.; Ahn, S.; Oh, K.-S. PredMS: A Random Forest Model for Predicting Metabolic Stability of Drug Candidates in Human Liver Microsomes. *Bioinformatics* **2022**, *38* (2), 364–368.
(66) Montanari, F.; Knasmüller, B.; Kohlbacher, S.; Hillisch, C.; Baierová, C.; Grandits, M.; Ecker, G. F. Vienna LiverTox Workspace-A Set of Machine Learning Models for Prediction of Interactions Profiles of Small Molecules With Transporters Relevant for Regulatory Agencies. *Front Chem* **2019**, *7*, 899.
(67) Schyman, P.; Liu, R.; Desai, V.; Wallqvist, A. vNN Web Server for ADMET Predictions. *Front Pharmacol* **2017**, *8*, 889.

## TABLE OF CONTENTS GRAPHIC